

# Effect of phosphorus on activity of hydrotreating catalyst of Maya heavy crude

S.K. Maity\*, J. Ancheyta, M.S. Rana, P. Rayo

*Instituto Mexicano del Petróleo, Eje Central Lázaro Cárdenas 152, Col. San Bartolo Atepehuacan, D.F. 07730, Mexico*

Available online 7 October 2005

## Abstract

The effect of phosphorus on physical properties of the catalyst and on activity of hydrotreating of Maya crude was studied in this work. Catalysts were prepared by the co-impregnation method. Alumina-titania binary oxide was used as a support material. The presence of phosphorus in the catalyst decreases the percentage of micropores, and it results in a decrease of specific surface area. Temperature program reduction (TPR) shows that phosphates reduce metal support interaction. It leads to the formation of polymolybdate phases in expense of strongly bonded tetrahedral molybdates. At higher P loading, polymolybdates may be present with quasi crystalline  $\text{MoO}_3$ . However, the TPR experiment is not sufficiently sensitive to distinguish several phases present on the catalysts used by the authors. A slight increment of HDM activity is observed, but HDS activity is lower in the P containing catalyst compared with the P free catalyst. The changes of physical properties of the spent catalysts are mainly due to the coke formation on the catalyst. The presence of phosphorus on hydrotreating catalysts inhibits coke formation during the hydrotreating reaction.

© 2005 Elsevier B.V. All rights reserved.

**Keywords:** Hydrotreating; HDM; HDS; Phosphorus; Deactivation; Maya crude

## 1. Introduction

To increase activity and stability of the hydrotreating catalysts, a large number of elements are used as additives. Among all these elements, phosphorous is mostly used as a third element in hydrotreating catalysts. Several effects in addition to phosphorous in hydrotreating catalysts have been reported in the literature.

With the increase of phosphorous content in alumina, an infra-red spectrum is shifted from 1119 to  $1152\text{ cm}^{-1}$  frequency region [1]. It explains the decrease of hydroxyl group in the alumina surface. Others also reported that with an increase of phosphorous concentration the  $\text{PO}_4^{3-}$  ion interacts with the hydroxyl group and forms di- and tri-phosphate [2]. It is reported that the structural properties of the catalysts have been changed due to the presence of phosphorous and that the effect depends on the properties of the support [1,3,4]. A decrease of surface area was observed with an increase in the phosphorous concentration. It was explained that P incorpora-

tion in alumina caused a decrease in micropores below 2.5 nm and an increase in mesopores, and hence, a decrease in surface area.

The phosphate ion present in the catalyst can modify the nature of the nickel in that catalyst. An increased amount of octahedral nickel is found in the phosphate modified catalyst [5]. It can change Type I Ni–Mo–S to Type II Ni–Mo–S, and therefore increases the HDT activity [6]. Phosphorous also inhibits the formation of  $\text{NiAl}_2\text{O}_4$  to increase the amount of a P–Ni–Mo heteropoly compound or form Mo–P tetrapoly and Ni-phosphate like compounds [7]. Studies also show that P increases the dispersion and reducibility of Co and Mo species [8–10]. Phosphorus increases the size of the  $\text{MoS}_2$  slab as well as the stacking number [11], but others have reported a decrease in the  $\text{MoS}_2$  length with the addition of phosphorus [12].

The effect of phosphorus content and preparation method on NiW/ $\text{Al}_2\text{O}_3$  catalyst was investigated by Atanasova et al. [3]. Thiophene HDS study shows that activity increases with increasing phosphorus content in the catalyst and it reaches a maximum at 2–3 wt.% of  $\text{P}_2\text{O}_5$ . The HDS activity decreases with further increase of phosphorus. It was also reported that a catalyst prepared by sequential method showed higher HDS activity than with co-impregnation method. The authors have

\* Corresponding author. Tel.: +52 55 91758422; fax: +52 55 91758429.  
E-mail address: [skumar@imp.mx](mailto:skumar@imp.mx) (S.K. Maity).

concluded that there is no structure-activity correlation due to the complex nature of the catalyst.

The formation of bulk  $\text{MoO}_3$  contributes to the decrease in the dispersion of Mo sulfide, which was further evidenced by the decrease in the amount of oxygen chemisorption as the phosphate content increased (10 wt.%  $\text{PO}_4$ ) [4]. Phosphate ions plug the micropore-mouth and hence decrease the surface area. Therefore, a phosphorus containing catalyst has fewer pores for adsorption of the molybdenum anion, causing molybdenum deposition to occur by precipitation. These precipitate molybdates are converted into crystalline  $\text{MoO}_3$  upon calcination. This decreases Mo dispersion and it results in a decrease of HDS activity.

From EXAFS study, Sajkowski et al. [13] suggested that there is no difference between the active phases of phosphorus free and phosphorus containing catalysts. Phosphorus increases hydrotreating activity and it may be due to weak interaction between active metal and support. Others have also supported the idea of the weak interaction between metal-support in P containing catalysts [14].

Kushiyaama et al. [15,16] reported that an appropriate concentration of P improved catalytic activity of heavy oil; however, an excess amount of it decreases activity. The authors assumed that P might interact strongly with the vanadium compound in the heavy feed, and it prevented deactivation of the active Mo species.

In summary, the primary role of phosphorus is to adsorb strongly with support, and thus to prevent a strong interaction of the active metals and the promoter with support. It results in the formation of well dispersed active species, and hence improved catalytic activity; but another study found a poisoning effect of P in the HDS activity. P may form P–O–Mo bonds at  $\text{MoS}_2$  edges and decrease activity [17].

Although there are several studies of phosphorus effect on catalysts for the hydrotreating of light fraction, there are very few studies of it on heavy oils. Therefore, the principal objective of the present investigation is to study the effect of phosphorus on catalyst structure, activity, and deactivation using Maya heavy crude as feed stock.

## 2. Experimental

### 2.1. Preparation of supports

Alumina-titania (AT, 95/5 wt. %) mixed oxide was prepared by a combination method of urea hydrolysis and pH variation. Three solutions of aluminum sulfate, titanium isopropoxide, and sodium aluminate were made in distilled water. A sufficient amount of urea was taken into a reactor vessel and was made into clear solution with water. The urea solution was heated at 90 °C with continuous stirring. The titanium solution was added to the reactor. The aluminum sulfate solution was added to the mixture until its pH reached 4. The mixture was aged 10 min. A basic solution of sodium aluminate was added until the mixture's pH reached 9, and then the mixture was aged for a duration of 10 min. The addition of acid and basic solutions was repeated a total of three times. The pH of the mixture was varied

from four to nine by adding acid and basic solutions of aluminum salts. The slurry was allowed 10 min in between the addition of acid and basic solutions. Finally, a base solution was added and the solution mixture was aged 3 h at a pH of 9. The slurry was then filtered and washed. The cake was used for making extruder. The extrudate was allowed to dry overnight at room temperature, after which it was dried at 160 °C for one day and calcined at 600 °C for 5 h.

### 2.2. Preparation of catalysts

The catalysts were prepared via the co-impregnation method. Appropriate amounts of ammonium heptamolybdate (AHM, Aldrich), cobalt nitrate (Aldrich), and/or phosphoric acid (Aldrich) were dissolved in water and the dried support (AT) was impregnated with the solution. One catalyst in this investigation contains only CoMo (P0), and the other three catalysts contain 0.4, 0.8, and 1.2 wt.% phosphorus in addition to the CoMo. These catalysts are referred to as P0.4, P0.8, and P1.2, respectively. Impregnated samples were dried 7 h at 120 °C and calcined for 3 h at 450 °C. All these catalysts contain 10 wt.% of  $\text{MoO}_3$  and 3 wt.% of CoO on the catalyst basis.

### 2.3. Characterization of catalyst

X-ray diffractograms were recorded on a SIEMENS D-500 model using  $\text{Cu K}\alpha$  radiation. The temperature programmed reduction (TPR) apparatus consisted of a quartz reactor and a thermal conductivity detector (TCD). Heating was performed with a tubular furnace regulated by a temperature controller. The reducing gas consisted of a mixture of 10%  $\text{H}_2$  in argon. The reducing gas mixture was purified by molecular sieves. 0.1 g of the catalyst weight was taken for each TPR experiment. Before each run, the baseline was stabilized at room temperature by passing a gas mixture at a flow rate of 25 ml/min. After stabilization, the sample was heated at 10 °C/min from room temperature to 1000 °C.

BET specific surface area, pore volume, and pore size distribution of fresh and spent catalysts were measured by nitrogen adsorption at 77 K (Automatic Micromeritics ASAP 2100). Metal contents of the spent catalysts were determined by an Atomic Absorption Spectrometer. The percentage of carbon was also measured on spent catalysts. The spent catalysts were washed with hot toluene by Soxhlet process and dried at 110 °C before carbon and metal analyses. Coke is defined in this work as being carbon content on spent catalysts.

### 2.4. Catalyst presulfiding

The oxide catalysts were sulfided in situ before an actual run began. Ten milliliters of oxide catalyst were loaded with an equal volume of diluent, non-porous silicon carbide (0.2 mm size). Both the catalyst and the diluent were mixed and divided into five parts. Each part of the mixture was individually loaded into the reactor and slightly tapped. The catalyst was then dried at 120 °C for 2 h at atmospheric pressure. After drying, the

Table 1  
Properties of Maya crude

Properties	Maya
API gravity	20.99
Sulfur (wt.%)	3.52
Nitrogen (wppm)	3006
Ramsbottom carbon (wt.%)	11.01
Asphaltenes (in C <sub>7</sub> ) (wt.%)	11.2
Ni + V (wppm)	318.9
TBP distillation (°C)	
IBP	19
10%	131
20%	201
30%	273
40%	352
50%	430
60%	509

catalyst was allowed to soak for 2 h at 150 °C. Light gas oil (LGO), which contained 1.7 wt.% of sulfur, was used for soaking. After soaking, the actual sulfiding agent, light gas oil with dimethyl disulfide (DMDS, 1 wt.%), was introduced. Sulfidation was performed at 28 kg cm<sup>-2</sup> pressure at two different temperatures. The first sulfidation was done at 260 °C for 3 h, and finally, the catalyst was sulfided at 320 °C for 5 h.

### 2.5. Catalyst activity test

Catalytic tests were performed in a high pressure fixed-bed micro-reactor in up flow mode. The experimental conditions were: total pressure, 54 kg cm<sup>-2</sup>; reaction temperature, 380 °C; liquid hourly space velocity (LHSV), 1.0 h<sup>-1</sup>; and hydrogen-to-hydrocarbon ratio, 356 m<sup>3</sup>/m<sup>3</sup>. A mixture of Maya heavy oil with hydrodesulfurized diesel (50/50 w/w) was used for the catalyst activity tests. The hydrodesulfurized diesel was used as a diluent since the micro-plant is not able to handle 100% Maya heavy crude. The properties of this crude are given in Table 1. The balances were taken after a stabilization of 9 h, and collected at a duration of 12 h each.

### 2.6. Analysis of feed and products

The total metals in the feed and products were measured by Atomic Absorption (ASTM D-5863). Sulfur and nitrogen were analyzed by X-ray fluorescence (ASTM D-4294) and chemiluminescence, respectively. Asphaltene is defined as the insoluble fraction in n-heptane (ASTM D-2007).

## 3. Results and discussion

### 3.1. X-ray diffraction (XRD)

X-ray diffractogram of pure support shows that the prepared binary oxide mainly contains alumina in gamma structure. A very weak peak is also observed at 2θ equal to 25.3° and is due to the presence of anatase titania. The XRD are studied in

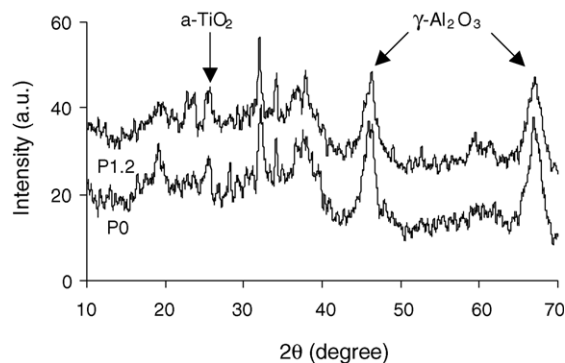


Fig. 1. Comparison of XRD diagrams of catalysts P0 and P1.2.

metals and phosphorus containing catalysts. Molybdenum oxide is well dispersed throughout the support since we do not observe any peak due to crystalline MoO<sub>3</sub>. In Fig. 1, we have compared the diffractograms of catalysts P0 and P1.2 to see if there is any change of texture due to the presence of P, and as shown, there is no considerable change in diffractogram.

### 3.2. Physical properties of catalysts

The physical properties of two catalysts, P0 and P1.2, are compared in Fig. 2 and Table 2. Figure shows that the pore size distributions of these two catalysts are almost identical except in the micro pore region. The total pore volume below 50 Å pore region has been reduced in the P containing catalyst and it causes loss of specific surface area (Table 2).

It was reported that phosphates block the micropores of the support, and therefore, specific surface area is decreased [1,3,4].



When molybdenum co-impregnates with phosphorus, phosphomolybdate anions ( $\text{P}_2\text{MoO}_{23}^{6-}$ ) are likely to form. These anions decompose into molybdate and phosphate during calcinations of the catalyst. Phosphate ions interact strongly with support, preferably with sites having micropores, and plug the pores.

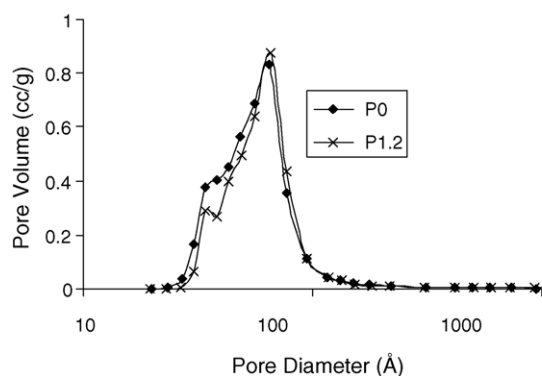


Fig. 2. Comparison of PSD of catalysts P0 and P1.2.

Table 2

Comparison of physical properties of phosphorus free (P0) and phosphorus (P1.2) containing catalysts

Properties	P0	P1.2
SSA (m <sup>2</sup> /g)	137	116
TPV (cc/g)	0.255	0.221
APD (Å)	74	76
PSD (vol. %)		
1000–500 (Å)	0.43	0.55
500–200 (Å)	1.01	1.09
200–100 (Å)	2.77	2.72
100–50 (Å)	51.13	58.8
<50 (Å)	44.66	36.84
<sup>a</sup> Carbon (wt.%)	11.9	10.2

<sup>a</sup> On spent catalyst.

### 3.3. Temperature programmed reduction (TPR)

The TPR profiles of pure alumina-titania support and supported catalysts are presented in Fig. 3. The binary mixed oxide support reduces at higher temperatures and temperature maxima ( $T_m$ ) appears at 778 °C. The reduction peak is sharp in nature. The reduction behavior of the molybdenum loaded catalyst is comparatively broad, and the main reduction peak  $T_m$  appears at a lower temperature of 661 °C. In addition, there is a small satellite peak at 691 °C. The broadness of this peak indicates that there may be more than one peak being superimposed. The promoted catalyst is reduced slightly at higher temperatures than the Mo/AT catalyst. However, the total peak area increases on the promoted catalyst. The reduction profiles of the phosphorus containing catalysts are complex and irregular. Catalyst P0.4 is reduced at 636 °C, and the total peak area is less than that of the promoted catalyst with

the only difference between these two catalysts being that the former has an additional 0.4 wt.% of P. The reduction peak also becomes broader in catalyst P0.4. In addition to 0.8 wt.% of P in catalyst P0.8, the  $T_m$  appears at 609 °C and the total peak area is slightly less than that of catalyst P0.4. Catalyst P1.2 is reduced at a higher temperature of 713 °C.

The TPR results demonstrate that alumina-titania support itself has reducible sites. It is true that the promoted catalyst has higher sites than the unpromoted one. The reduction behaviors of P containing catalysts are more complex. A comparison of total reducible area shows that a phosphorus containing catalyst has less reducible area than a non-phosphorus catalyst. It has been discussed earlier that phosphate strongly interacts with support and that it leads a weak interaction of oxide precursors with support. This weaker interaction results in the formation of polymolybdate phases. When interaction is reduced to a certain level, some of the polymolybdates are converted to crystalline MoO<sub>3</sub>. Therefore, a plausible explanation for the lower  $T_m$  of P containing catalysts is that the formation of polymolybdate phases in expense of tetrahedral molybdate which has stronger interaction with support. However, shifting of the  $T_m$  of P1.2 at a higher temperature remains unresolved. It may be possible that the high P containing catalyst has crystalline MoO<sub>3</sub> with polymolybdates. The crystalline MoO<sub>3</sub> reduces at higher temperature. The reduction profile of catalyst P1.2 may be superimposed of reduction peak of polymolybdates and reduction peak of the crystalline MoO<sub>3</sub>, but our XRD results do not support it, i.e., we did not observe any peak that corresponded to crystalline MoO<sub>3</sub>. It may be possible that this crystalline MoO<sub>3</sub> is below the detection level of XRD experiment. It can be also explained in other way that this is not exactly crystalline MoO<sub>3</sub>; it may be aggregates of polymolybdate or quasi crystalline MoO<sub>3</sub>, which was also observed by Cruz et al. [18]. At this juncture, it is worthwhile to mention that the catalytic system used in this work is complex in nature. It contains alumina, titania, molybdenum, cobalt, and phosphorus. It is very obvious the presence of the different reducible components. The TPR experiment is not efficient enough to distinguish these different reducible components.

The presence of total reducible species in phosphorus containing catalysts is less than that of a phosphorus free catalyst. Two explanations were given by Mangnus et al. [19]: the first one is that a part of Mo, which adsorbed as phosphomolybdate, does not decompose fully upon calcinations, and the second explanation is that the phosphomolybdate complex reacts with AlPO<sub>4</sub> and the Al-O-Mo species, and these Mo species remain in contact with AlPO<sub>4</sub> upon calcination. In the case presented here, the second explanation can be discarded because no reduction peak due to AlPO<sub>4</sub>, which generally appears at around 924 °C, was observed. Hence, the reduction of reducible Mo species in P containing catalysts may be due to some Mo remaining in the phosphomolybdate structure. The reduction of phosphomolybdates was very difficult, as reported by Van Veen et al. [20].

The above results demonstrate the complexity of the multicomponent system. It is also important to note here that the used support consists of binary oxides of alumina and

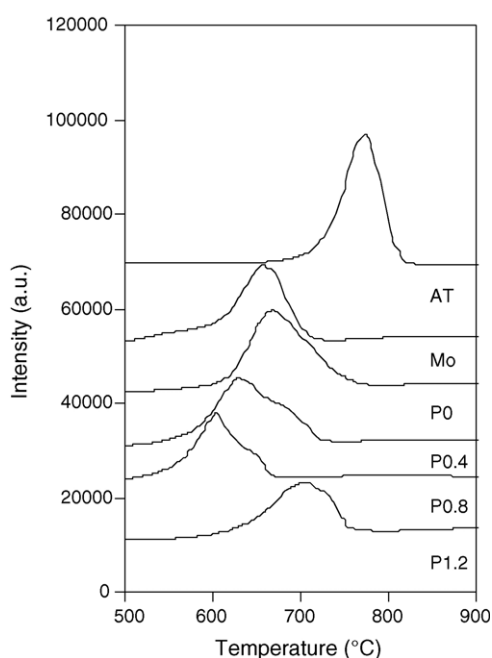


Fig. 3. TPR patterns of catalysts.

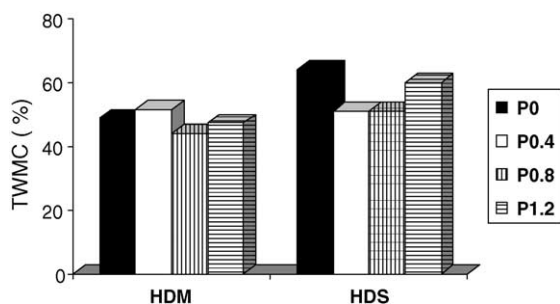


Fig. 4. Percentage of time weighted mean conversions of catalysts.

titania. The affinity of interaction of oxide precursors with alumina and titania is different and it leads to a more complex system, and hence, the reduction behavior.

### 3.4. Catalytic activity

The hydrodemetallation (HDM) and hydrodesulfurization (HDS) are studied in a micro-reactor in upflow mode, and conversions of three catalysts are compared in Fig. 4. In this figure, time weighted mean conversion (TWMC) is calculated using the following equation [10]:

$$\text{TWMC} = \frac{\sum_{i=1}^N x_i t_i}{\sum_{i=1}^N t_i}$$

where  $x$  is the conversion,  $t$  the time (duration of balance), and  $N$  the number of balances. Although initial conversions of the catalysts are high, they decrease sharply with time. Therefore, TWMC is more appropriate to discuss these results, since it takes into account the time factor into the conversion. This approach has two benefits: it allows the averaging of variable data over a number of balances to obtain a more real performance, and it gives less weight to the initial conversion.

In Fig. 4, the effect of phosphorus on HDT reactions is compared. The effect on HDM is different than that on HDS. The HDM activity slightly increases with the addition of P; however, the HDM activity of P0.8 is less than the P0 catalyst.

The hydrodesulfurization activity is less on phosphorus containing catalysts than on the phosphorus free catalyst.

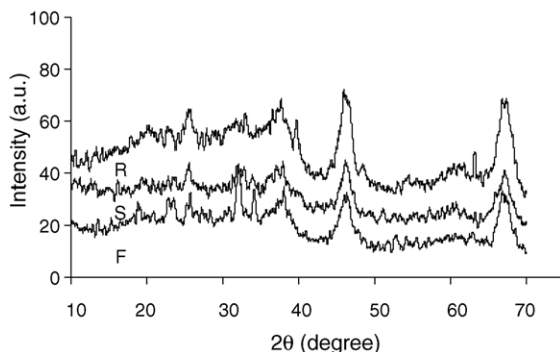


Fig. 5. XRD diagrams of fresh (F), spent (S) and regenerated (R) catalyst P0.8.

Table 3

Physical properties of fresh (F), spent (S) and regenerated (R) catalyst P0.8

Properties	F	S	R
SSA (m <sup>2</sup> /g)	128	89	111
TPV (cc/g)	0.247	0.112	0.201
APD (Å)	77	50	72
PSD (vol.%)			
1000–500 (Å)	0.64	0	0
500–200 (Å)	0.99	1.69	1.95
200–100 (Å)	7.45	3.39	6.95
100–50 (Å)	69.5	25.24	64.9
<50 (Å)	21.42	69.68	26.2

Among the three P containing catalysts, P1.2 shows higher HDS activity.

In the authors' previous work, the synergic effect of phosphorus was clearly observed [10], indicating that its effect is support sensitive, i.e., in different support (maybe depending on its acidic) phosphorus acts differently.

No linear correlation of catalytic activity with catalyst properties was observed. Even the effect of phosphorus is different for HDM and HDS reactions. The catalysts used contain active metal (Mo), promoter (Co), and additive (P), such that it is a multicomponent system and each component has its own effect on HDT reactions. Consequently, the total effect of this type of catalyst on HDT reaction is complex. Therefore, more investigation is needed in order to make a clear conclusion.

### 3.5. Catalyst deactivation

X-ray diffractograms of the spent catalysts were also studied and only the diffractogram of catalyst P0.8 is presented in Fig. 5. In this figure, the fresh and regenerated catalysts are compared. The spent catalyst was regenerated in control flow of air at 500 °C for 4 h. No drastic change in diffractograms of spent and regenerated catalysts can be observed. It means that the size of metal sulfides (vanadium and nickel) may be below the 40 Å, detection level in XRD. A similar effect is observed in the other three catalysts.

Physical properties of the spent catalysts were also measured. In Table 3, specific surface area and total pore volume, and metal deposition of spent catalyst P0.8 are given.

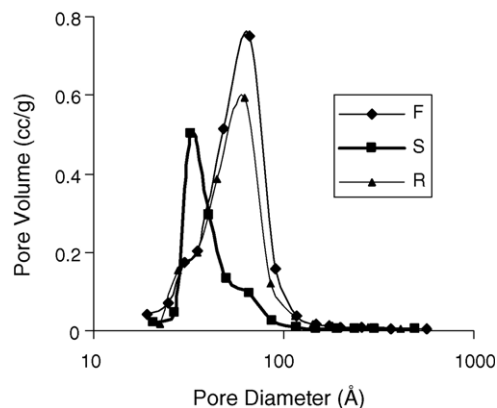


Fig. 6. Pore size distributions of fresh, spent and regenerated catalyst P0.8.



Those properties of fresh and regenerated catalyst of the same are also included in this table. The pore size distributions of fresh, spent, and regenerated catalysts of P0.8 are also presented in Fig. 6, which clearly demonstrates the change of pore size distribution. PSD of the spent catalyst is shifted to a lower pore region compared with the fresh catalyst. PSD of the regenerated catalyst is almost identical to the fresh catalyst expected total pore volume. TPV of the former is reduced in the spent catalyst.

Carbon and metals, particularly vanadium and nickel, are deposited into the catalyst pore during heavy oil hydrotreating. During regeneration, carbon has left out from the pores as carbon dioxide, but metals remain into the pores. Thus, the above results explain that the changes of the physical properties of the spent catalyst are mainly due to coke deposition.

In Table 2, carbon deposition is presented, and it indicates that the coke formation is less on the P containing catalyst. The phosphate can modify the catalyst in several ways. It interacts strongly with support and hence reduces the possibility of direct interaction of coke precursors and support. It is also reported in the literature [21] that phosphorus decreases the number of strong acid sites of the catalyst. These acid sites facilitate the coke formation on the catalyst. Therefore, this may be another reason for inhibition of coke formation in P-catalysts. Kushiyama et al. [15] stated that phosphorus may interact with vanadium in heavy feed and that prevents deactivation of the catalyst.

Activities of all four catalysts are also studied with time-on-stream, and results are presented in Fig. 7. It is observed that activities decrease with time; however, the rates of deactivation are different for the four catalysts. Catalyst P0.4 shows higher

initial HDM activity as well as good stability with run of operation. Although initial HDM activity of catalyst P0 is a little higher than catalyst P0.4, the activity of the former falls gradually.

The rate of deactivation of the HDS reaction for catalyst P1.2 is less compared with the other P containing catalysts P0.8 and P1.2.

#### 4. Conclusions

The effect of phosphorus on textural properties of the catalyst is observed. The percentage of micropores is reduced when adding phosphorus, and it causes a decrease in specific surface area. TPR results show that the promoted catalyst has more reducible species. TPR profiles of phosphorus containing catalysts are broad in nature. It can also be speculated from our TPR results that phosphorus containing catalysts have polymolybdate phases, and these phases may be aggregated at a higher P content. The effect of phosphorus is selective on HDM and HDS reactions. Though there is slight promotional effect of P on HDM activity, HDS activity is low in P containing catalysts compared with the P free catalyst. The deactivation study shows that the changes in physical properties of the spent catalyst are mainly due to coke deposition on catalyst pore-mouth. Phosphorus inhibits coke formation on the catalyst surface.

#### Acknowledgment

The authors would like to thank the Instituto Mexicano del Petroleo for the financial support.

#### References

- [1] A. Spojakina, S. Damyanova, L. Petrov, *Appl. Catal.* 56 (1989) 163.
- [2] F.A. Cotton, G. Wilkinson, in: Limusa (Ed.), *Inorganic Chemistry* 20 (1975) 43.
- [3] P. Atanasova, T. Tabakova, Ch. Vladov, T. Halachev, A. Lopez Agudo, *Appl. Catal. A* 161 (1997) 105.
- [4] S.I. Kim, S.I. Woo, *J. Catal.* 133 (1992) 124.
- [5] P. Atanasova, T. Halachev, J. Uchetil, M. Kraus, *Appl. Catal.* 38 (1988) 235.
- [6] S. Eijisbouts, J.N.M. van Gestel, J.A.R. van Veen, V.H.J. de Beer, R. Prins, *J. Catal.* 131 (1991) 412.
- [7] K. Gishti, A. Iannibello, S. Marengo, G. Morelli, P. Tittarelli, *Appl. Catal.* 12 (1984) 381.
- [8] A. Morales, M.M. Ramirez, M.M.R. de Agudelo, *Appl. Catal.* 23 (1986) 23.
- [9] J.M. Lewis, R.A. Kydd, *J. Catal.* 136 (1992) 478.
- [10] S.K. Maity, J. Ancheyta, L. Soberanis, F. Alonso, *Appl. Catal. A* 253 (2003) 125.
- [11] P. Zeuthen, P. Blom, F.E. Massoth, *Appl. Catal.* 78 (1991) 265.
- [12] J. Ramirez, V.M. Castaño, C. Leclecq, A. López-Agudo, *Appl. Catal. A* 83 (1992) 251.
- [13] D.J. Sajkowski, J.T. Miller, G.W. Zajac, *Appl. Catal.* 62 (1990) 205.
- [14] M. McMillan, J.S. Brinen, G.L. Haller, *J. Catal.* 97 (1986) 243.
- [15] S. Kushiyama, R. Aizawa, S. Kobayashi, Y. Koinuma, I. Uemasu, *Appl. Catal.* 63 (1990) 279.
- [16] S. Kushiyama, R. Aizawa, S. Kobayashi, Y. Koinuma, I. Uemasu, H. Ohuchi, *Ind. Eng. Chem. Res.* 30 (1990) 107.

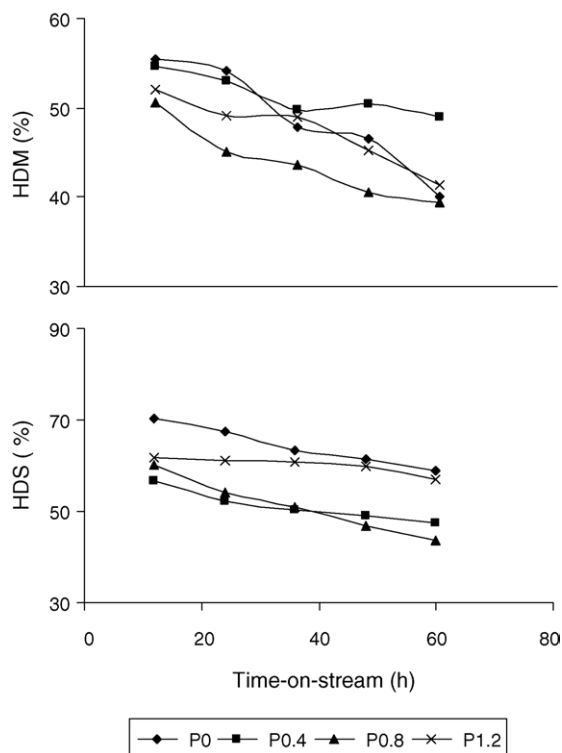


Fig. 7. Percentage of conversions with time-on-stream.

- [17] J.P.R. Vissers, S.M.A.M. Bouwens, V.H.J. de Beer, R. Prins, *Am. Chem. Soc. Div. Pet. Chem. Prepr.* 31 (1986) 227.
- [18] J. Cruz, M. Avalos-Borja, R. López Cedero, M.A. Bañares, J.L.G. Fierro, J.M. Palacios, A. López-Agudo, *Appl. Catal. A* 224 (2002) 97.
- [19] P.J. Mangnus, J.A.R. Van Veen, S. Eijssbouts, V.H.J. de Beer, J.A. Moulijn, *Appl. Catal.* 61 (1990) 99.
- [20] J.A.R. van Veen, O. Sudmeijier, C.A. Emeis, H. de Wit, *J. Chem. Soc. Dalton Trans.* (1986) 1825.
- [21] A. Stanislaus, M. Abasi-Halabi, K. Al-Dolama, *Appl. Catal.* 39 (1988) 239.